JOURNAL OF CATALYSIS 63, 346–354 (1980)

Gas Phase Hydrogenation of Benzene on Supported Nickel Catalyst

H. A. FRANCO AND M. J. PHILLIPS

Department of Chemical Engineering and Applied Chemistry, University of Toronto, Toronto, Ontario, M5S 1A4, Canada

Received March 16, 1979; revised August 23, 1979

The kinetics of benzene hydrogenation over a nickel–kieselguhr catalyst was studied in a differential flow microreactor. Temperatures ranged from 392.2 to 468.2 K, benzene partial pressures from 22.66 to 280 Pa, hydrogen partial pressures from 72.39 to 122.79 kPa, and cyclohexane partial pressures from 5.33 to 40 Pa. Cyclohexane was the only product of the reaction. The results were consistent with a mechanism in which all hydrogen addition steps were assumed to have the same rate constant and to form a set of slow steps. This mechanism could predict the maximum in the hydrogenation rate observed at about 458 K. A temperature-programmed desorption study of hydrogen chemisorbed on the catalyst indicated a number of desorption peaks between 358 and 600 K, one of which was coincident with the rate maximum.

INTRODUCTION

In spite of the fact that benzene hydrogenation over transition metals is, to some extent, a well-known reaction, its mechanism and kinetic behavior are still far from being completely understood. The reaction proceeds over most Group VIII metals at reasonable rates, giving, in general, cyclohexane as the only product when moderate temperatures are employed and cracking products above 623 K. Considerable attention has been paid to the kinetics of the benzene hydrogenation on nickel catalysts (*1–9*) since, industrially, standard nickel catalysts are used for the gas-phase hydrogenation and Raney-nickel for the liquid-phase hydrogenation (*10*).

Most of the authors who have studied this reaction at temperatures below 373 K reported reaction orders with respect to benzene pressure of 0.1 to 0.3 (*3, 5, 6, 8, 9, 11–13*), while reaction orders with respect to hydrogen pressure were found to lie between 0.5 and 0.7 (*3–5, 8, 9, 11, 14–17*). At higher temperatures (up to 483 K) the temperature dependence shown by the order becomes more significant; for hydrogen the order increased from 1 to 3 (*3, 5, 8, 9, 18*).

Less agreement exists concerning the effect of cyclohexane with some investigators reporting an inhibiting action (*3, 4, 12, 13*).

Reported activation energies for benzene hydrogenation vary widely below 458 K. Although most values fall between 41 and 58 kJ mol^{-1} (*12, 18, 19, 23*) for supported catalyst, some extreme values of 67 kJ mol^{-1} (*3, 13*) and 94.2 kJ mol^{-1} (*28*) have been observed.

A maximum in the hydrogenation rate on nickel catalyst around 453 K is mentioned by several workers (*3, 4, 9, 12, 20, 21*). Similar results have been reported for other metals (*25, 26*). Suggested explanations for this phenomenon include: poisoning, decreasing reactant adsorption, or decreasing concentration of intermediate species.

Widely different mechanisms and kinetic equations have been proposed (*3, 7, 11, 23, 24, 27, 28*). Recently van Meerten and Coenen (*29*) based on the work of Snagovskii (*8*) have proposed three possible mechanisms, two of them having an adjustable rate-determining step and the third, a set of slow steps.

EXPERIMENTAL METHODS

Apparatus (*Fig. 1*). The gas phase hydrogenation was performed in a differential flow reactor. The microreactor, (A), con-

0021-9517/80/060346-09$02.00/0

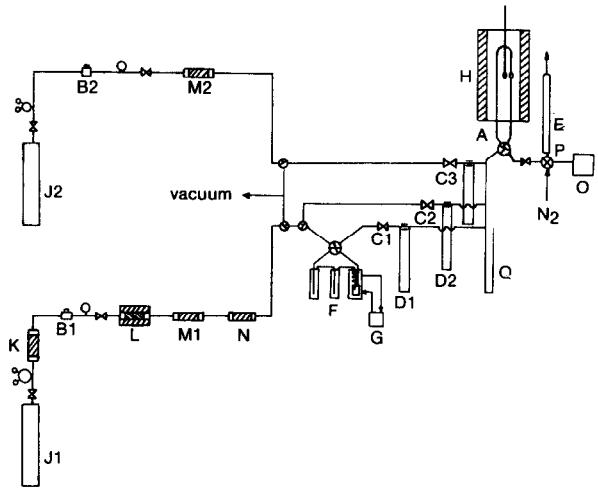

FIG. 1. Schematic diagram of the experimental apparatus for kinetic studies.

sisted of a 2.5-mm-i.d. Pyrex tube with a fritted glass insert on which the catalyst was supported. Reproducible flow rates were obtained by pressure regulation valves (B1) and (B2), connected to fine metering valves (C1), (C2), and (C3). Further reduction was achieved via capillary flowmeters (D1), (D2), and (D3). The reactor gas effluent was measured by a soap-bubble flowmeter (E). A carburettor, (F), composed of two evaporators and one condenser, provided with fairly good precision the benzene vapor at the pressure corresponding to the condenser temperature. The temperature of the condenser was kept at 289.2 ± 0.01 K by means of a constant temperature circulating system (G). The microreactor was placed inside an electric tubular furnace, (H). The temperature of the furnace was controllable to within ± 0.01 K by an adjustable microset thermoregulator, (I).

Materials. Cyclohexane and thiophene-free benzene with a certified purity of 99 mole% obtained from Fisher Scientific Co. were used without further purification.

Hydrogen from the cylinder, (J), passed through a Deoxo unit, (K), then through copper catalyst, (L), at 523 K, a molecular sieve trap, (M), and Ascarite, (N). Helium from the cylinder, (J2), passed through a molecular sieve trap, (M2), before being used.

Dark gray tablets containing 55% nickel as nickel oxide on kieselguhr (Harshaw, Ni-0102, T 1/8″) were used for all experiments. The catalyst was ground and a sample was taken from the 44 to 37 μm fraction. The surface area by BET nitrogen adsorption was 123.24 $m^2 g^{-1}$.

Analysis of feed and reaction products. Reactor effluent samples were injected into a gas chromatograph, (O), via a microvolume sampling valve, (P). The gas chromatographic column, 2 m in length, 1.5 mm i.d. Teflon, packed with 15% Carbowax 20 M on Chromosorb W AW, 250–177 μm, gave a good separation of cyclohexane and benzene at 323 K.

Procedure. A 1-mg sample of nickel catalyst diluted with 2 mg of ground Vycor, also from the 44 to 37 μm fraction, was loaded on the fritted glass of the microreactor.

After evacuation of the purification train for up to 1 hr, a hydrogen flow of 20 cm^3 (STP) min^{-1} was established through the reactor in order to reduce the catalyst. The reactor temperature was then slowly increased to 653 K and kept constant for 12 hr. This reduction procedure was carried out between each series of runs to regenerate the catalyst. A total gas flow of 995 cm^3

(STP) min^{-1} was sufficient to avoid external mass resistance from the reacting gases to the catalyst surface. A total pressure of 122.92 kPa, indicated in the manometer, (Q), was set for each experiment.

Since it has been observed from previous experiments that a series of runs, in which different sets of conditions were established, resulted in some loss of activity, the method proposed by Yates *et al.* (*30*) was used to bracket all rate measurements with measurements at a standard set of conditions. The catalyst was discarded when a third regeneration was necessary and replaced with fresh material.

RESULTS AND DISCUSSION

Variation in the partial pressure of benzene was carried out at temperatures from 392.2 to 468.2 K, keeping the partial pressure of hydrogen constant. The results are shown in Fig. 2. The order of reaction with respect to benzene pressure ranged from about 0.6 to 0.8, depending upon both temperature and benzene pressure.

It can be seen that an increase in benzene partial pressure, at any particular temperature, increased the rate of reaction. Of special interest is the evidence of a maximum in the rate of hydrogenation which occurs around 458 K. This can clearly be observed in Fig. 3, where the logarithm of reaction rate is plotted versus reciprocal temperature for four different partial pressures of benzene.

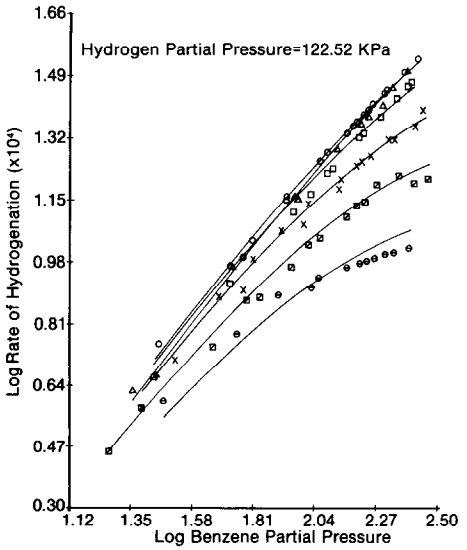

FIG. 2. Effect of the partial pressure of benzene (Pa) on the rate of hydrogenation (g · mol [g · cat.]$^{-1}$ min^{-1}). ○, 453.2 K; △, 468.2 K; □, 438.2 K; ×, 423.2 K; ⊠, 408.2 K; ⊖, 393.2 K.

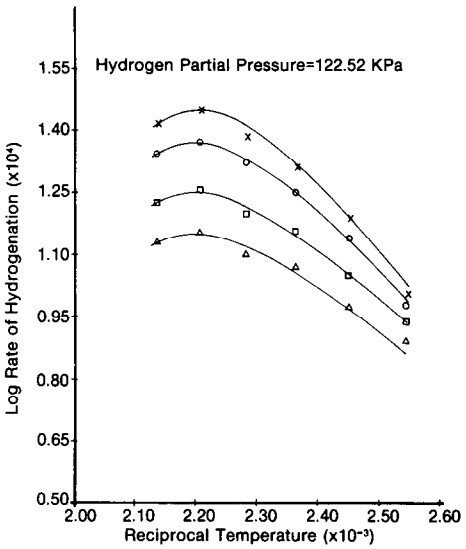

FIG. 3. Effect of the temperature (K) on the rate of hydrogenation (g · mol [g · cat.]$^{-1}$ min^{-1}). ×, p_B = 199.9 Pa; ○, p_B = 162.6 Pa; □, p_B = 113.3 Pa; △, p_B = 86.6 Pa.

Unusual catalyst poisoning must be ruled out as a cause of this maximum since reaction rates measured for decreasing temperatures (468.2 to 438.2 K) were the same, within experimental error, as those obtained for increasing temperatures. A diffusion limitation might be considered to cause this maximum, but the small particle size of catalyst used together with the low conversions obtained (about 1%) make the effectiveness factor close to unity and diffusion resistance negligible. Nor can this phenomenon be ascribed to an approach to thermodynamic equilibrium since the high gas flow rate removed the cyclohexane quickly thus favoring the forward reaction.

The temperature-programmed desorption (TPD) experiments (Fig. 6) showed that the amount of chemisorbed hydrogen

on the surface decreased as temperature increased. This may suggest that an insufficient amount of adsorbed hydrogen could be the cause of the reaction rate decrease at higher temperatures.

A stream of purified helium was used as diluent to change the partial pressure of hydrogen. Benzene partial pressure and reaction temperature were kept constant in each run. Figure 4 shows that the order of reaction with respect to hydrogen pressure depends upon both temperature and hydrogen pressure. In this case the order ranged from, approximately, 0.5 to 0.7

Experiments were performed with some standard mixtures containing small concentrations of cyclohexane to determine whether the product caused any inhibition in hydrogenation rate. Partial pressures of hydrogen and benzene were kept constant at 422.2 K. No effect of cyclohexane pressure was observed as Fig. 5 illustrates. These results are entirely reasonable since the reactor behaved differentially in the whole range of cyclohexane pressures used and under these circumstances, it is expected that small changes in the partial pressure of cyclohexane would have no influence on the hydrogenation rate. Since in the differential reactor conversions were very low and the partial pressure of cyclohexane produced has to be calculated from the difference between the total amount of cyclohexane in the reactor gas effluent and that of the feed, initial partial pressures of cyclohexane beyond 40 Pa were not considered.

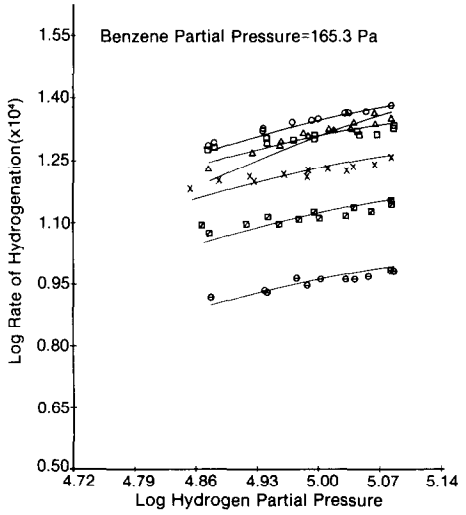

FIG. 4. Effect of the partial presure of hydrogen (Pa) onthe rate of hydrogenation (g · mol [g · cat.]$^{-1}$ min^{-1}). ○, 453.2 K; △, 468.2 K; □, 438.2 K; ×, 423.2 K; ⊠, 408.2 K; ⊖, 393.2 K).

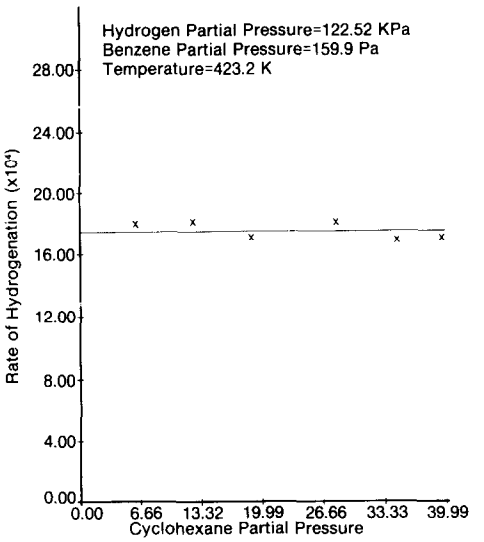

FIG. 5. Effect of the partial pressure of cyclohexane (Pa) on the rate of hydrogenation (g · mol [g · cat.]$^{-1}$ min^{-1}).

Reaction Mechanism

A functional optimization by Rosenbrock's method of hill-climbing (*31, 32*) was used to treat the extensive data, 164 independent runs. This computer program involves a minimization of the function

$$G = \sum_{i=1}^{164} \left| \frac{\log r^i_{\text{exp}} - \log r^i_{\text{cal}}}{\log r^i_{\text{exp}}} \right| \qquad (1)$$

by variation of the values for the constants in possible rate equations. In total, 12 equations were tried. That of Badilla-Ohlbaum *et al.* (*25*) which had successfully correlated data in the same pressure range on a singly promoted iron catalyst suggested that the rate controlling step is the simulta-

neous reaction of three molecules of dissociatively chemisorbed hydrogen with one molecule of adsorbed benzene. That of Kehoe and Butt (*6*) developed for a 58 wt% nickel on kielseguhr catalyst described a Rideal mechanism with the molecular addition of hydrogen to absorbed benzene.

Van Meerten and Coenen (*29*), working on the same basis as Snagovskii (*8*), suggested three possible mechanisms, all of them considering the hydrogenation of benzene as a sequence of hydrogen atom additions to adsorbed benzene and partially hydrogenated benzene molecules, where: (a) the hydrogen addition steps are in equilibrium up to a rate-determining step and further hydrogen addition steps are faster; (b) all hydrogen addition steps have the same rate constant; and (c) the hydrogen addition steps are equilibria up to a rate-determining step, further addition steps having the same rate constant as this step. The first of these mechanisms leads to five equations, the third to four, and the second to only one.

Of the 12 equations, that one derived on the basis of van Meeten and co-workers' second, (b), mechanism (*29*) provided the best fit for the data. That is,

$$r = \frac{k_+(b_{H_2}p_{H_2})^{1/2}\, b_B p_B A^5}{[1 + (b_{H_2}p_{H_2})^{1/2}][b_B p_B(6A^5 + 5A^4 + 4A^3 + 3A^2 + 2A + 1) + (A^5 + A^4 + A^3 + A^2 + A + 1)]} \quad (2)$$

where k_+ is the rate constant for the addition of an adsorbed H atom to an adsorbed partially hydrogenated benzene molecule and is equal to k_-, the rate constant for the reverse reaction, b_{H_2}, and b_B are the adsorption equilibrium constants for hydrogen and benzene; and A equals $(k_+/k_-)(b_{H_2}p_{H_2})^{1/2}$.

Equation (2) was the only one of the 12 to give physically acceptable values for all the constants. Values for the activation entropy, ΔS^*, and the activation enthalpy, ΔH^*, of the forward and reverse hydrogenation steps and the adsorption entropies and enthalpies for hydrogen and benzene as defined by van Meerten and Coenen (*29*) are listed in Table 1. It may be noted that the value of the activation enthalpy of the kinetic rate constant is very close to the values reported for the reaction over other catalysts (*4–8, 25, 29*). The adsorption enthalpy of benzene is similarly close to values reported on nickel (*6, 25, 29*) and on other surfaces (*33*). The fact that the adsorption enthalpy of hydrogen is lower than that of benzene suggests that hydrogen is more weakly adsorbed on the surface than is benzene. This is in agreement with the remarks made by Basset *et al.* (*34*).

The curves in Figs. 2, 3, and 4 were developed from Eq. (2) and are in good agreement with experimental data (the minimum of the function (1) was $G = 0.0155$ and the standard deviation, 6.22%).

Surface coverages calculated by applying the stationary state condition to the whole group of slow steps (absorption of benzene, dissociative adsorption of hydrogen, the six

TABLE 1

Results Obtained from Eq. (2)[a]

	kJ mol^{-1}	J mol^{-1} K^{-1}	Benzene sites (g-cat.)$^{-1}$
ΔH_+^*	55.385		
ΔS_+^*		−43.04	
ΔH_-^*	94.408		
ΔS_-^*		−12.89	
ΔH_B	−33.328		
ΔS_B°		−43.16	
ΔH_{H_2}	−24.129		
$\Delta S_{H_2}^\circ$		−144.82	
n_B			7.7×10^{18}

[a] Where: $k_+ = n_B \frac{kT}{h} \exp(\Delta S_+^*/R - \Delta H_+^*/RT)$

$k_- = n_B \frac{kT}{h} \exp(\Delta S_-^*/R - \Delta H_-^*/RT)$

$b_H = \exp(\Delta S_{H_2}^\circ/R - \Delta H_{H_2}/RT)$

$b_B = \exp(\Delta S_B^\circ/R - \Delta H_B/RT)$.

hydrogen addition steps, and the desorption of cyclohexane) are given in Table 2. In particular, since benzene and hydrogen are considered noncompetitive, the surface occupied by benzene and hydrogenated species is given by $\theta_x + \sum_{n=0}^{6} \theta_{(C_6H_{6+n})_{ad}} = 1$ and that by hydrogen is given by $\theta_y + \theta_{(H)ad} = 1$. The total surface coverage of benzene and hydrogenated species decreases with increasing temperature from 0.51 to 0.17 implying reversible adsorption of benzene. The coverage of each of $(C_6H_6)_{ad}$ through $(C_6H_{11})_{ad}$ is effectively equal at the lower temperatures studied although at higher temperatures, the coverage as calculated becomes significantly less for the more highly hydrogentated species.

An interesting observation is that the decrease in the surface coverage by hydrogen does not influence, as much as has been thought, the maximum obtained in the rate of hydrogenation. Careful study of Table 2 will show that the $\theta_{(C_6H_{11})_{ad}}$ at 468.2 K has been reduced about 77% with respect to its value at 398.2 K, while the $\theta_{(H)ad}$ has been reduced by only 43% in the same range of temperature. The surface coverage of benzene itself has been decreased appreciably, which may be caused by the low partial pressure of benzene being used.

Therefore, the appearance of a maximum in the rate of hydrogenation may be a consequence of two effects: first, the increasing values for the rate constant k_+ with temperature, and second, the reduction in the surface coverage of $(C_6H_{11})_{ad}$, which is more rapid at temperatures above 458.2 K. However, it is possible that the decreasing surface coverage of hydrogen, shown by TPD experiments and also calculated in Table 2 may play a secondary role in accounting for this phenomenon.

A temperature-programmed desorption (TPD) apparatus, similar to the one developed by Cvetanovic and Amenomiya (*36*), was used. A 0.9780-g sample of the same catalyst size fraction taken for the kinetic study was used in the hydrogen chemisorption experiments.

Hydrogen, purity 99.5%, was passed through copper gauze at 623 K and a charcoal trap immersed in liquid nitrogen and was stored in a 5-liter reservoir. This same hydrogen could also be fed to the reactor for catalyst reduction. Prepurified nitrogen, purity 99.998%, used as carried was passed through a molecular sieve trap and a liquid nitrogen trap filled with 6-mm-diameter glass beads.

Before each run, the catalyst was treated as follows: after evacuation of the purification train and reactor for up to 1 hr, a hydrogen flow of 300 cm^3 (STP) min^{-1} was established through the reactor in order to reduce the catalyst. The reactor temperature was slowly increased to 653 K and kept at that temperature for 12 hr. The temperature was then increased to 923 K and the catalyst evacuated for 1 hr. The catalyst was finally cooled to the actual temperature

TABLE 2

Surface Coverage

Temp. (K)	θ_X	$(C_6H_6)_{ad}$	$(C_6H_7)_{ad}$	$(C_6H_8)_{ad}$	$(C_6H_9)_{ad}$	$(C_6H_{10})_{ad}$	$(C_6H_{11})_{ad}$	$(H)_{ad}$	θ_Y
398.2	0.490	0.086	0.086	0.086	0.086	0.085	0.082	0.007	0.993
408.2	0.553	0.075	0.075	0.075	0.075	0.975	0.071	0.006	0.994
418.2	0.611	0.066	0.066	0.066	0.066	0.065	0.060	0.006	0.994
428.2	0.665	0.057	0.057	0.057	0.057	0.056	0.050	0.005	0.995
438.2	0.713	0.050	0.050	0.049	0.049	0.048	0.041	0.005	0.995
448.2	0.756	0.043	0.043	0.043	0.042	0.041	0.033	0.005	0.995
458.2	0.795	0.037	0.037	0.037	0.036	0.033	0.026	0.004	0.996
468.2	0.829	0.032	0.032	0.031	0.030	0.027	0.019	0.004	0.996

of adsorption while pumping was continued. After adsorption took place, the catalyst was again evacuated before the carrier gas was diverted into the reactor. The temperature controller-programmer allowed the temperature to increase continuously from room temperature to 923 K at a rate of 5 K/min although there was a time lag of about 5 min, at the beginning of the run, before that rate was reached. The carrier gas flow was then set at 40 cm^3 (STP) min^{-1} and no change in the base line was observed over the entire range of scanned temperatures. Since the reactor had a volume of only 1 cm^3, the average residence time in the catalyst bed was about 0.05 sec.

Adsorption of hydrogen was always rapid since no change of pressure could be observed after a few minutes. In Fig. 6, curve 1, hydrogen was adsorbed at 298 K for 5 hr at 122.52 kPa and then evacuated at the same temperature for 5 min. The first peak appeared at a temperature of 358 K followed by a smaller peak at about 453 K; this may suggest that the peak appearing at the higher temperature (453 K) represents a stronger adsorption and therefore a smaller activation energy of adsorption than that at the lower temperature. The peak at 453 K did not change position in the desorption chromatogram when the adsorption temperature was changed to 635 and 775 K, curves 2 and 3, respectively, indicating that this type of adsorption has readily occurred at lower temperatures and developed as the temperature of adsorption increased.

Curve 2 was obtained by adsorbing hydrogen at 122.52 kPa for 30 min at 635 K, cooling to 298 K in the presence of hydrogen (the cooling process took an average of 15 min), and then adsorbing at 398 K for another 5 hr at the same pressure. The peak previously obtained at 358 seemed to have shifted to 393 K. The remaining part of this curve showed a large peak at 458 K instead of 453 K and smaller peaks at 533, 568, and 603 K.

The conditions for adsorption in curve 3 were: at 122.52 kPa for 30 min at 775 K and at 298 K for 1.5 hr. A larger peak at 533 K, instead of two smaller peaks at 533 and 568, distinguished this desorption chromatogram from that represented in curve 2. Since the first two peaks in curves 2 and 3 were almost equal, the sites corresponding to these two types of adsorption were already saturated at 635 K or even below. However, the peak at 533 K in curve 3 was increased appreciably indicating that saturation had not been achieved.

The total area under these desorption chromatograms coincided within ±6% indicating that the amount of hydrogen desorbed was the same (within experimental error). As seen in Fig. 6, almost all of the hydrogen has been desorbed at 823 K. It

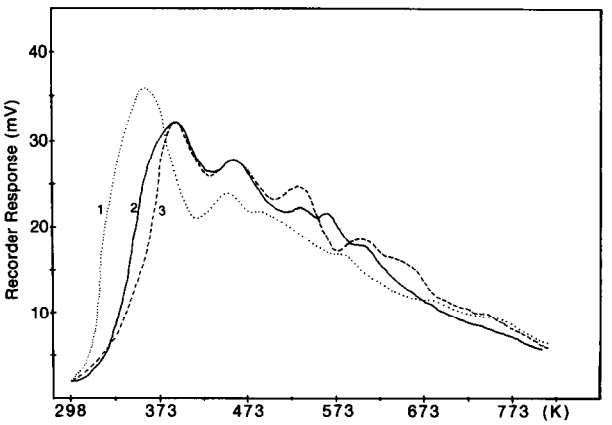

FIG. 6. Temperature-programmed desorption spectra of hydrogen.

should be noted that the base line is regained by about 923 K. Consideration of all three curves suggests that the first peak obtained at 358 K, curve 1, shifted to a higher temperature as adsorption temperatures increased. These two facts may be explained if the sites for the adsorption of hydrogen are already saturated at room temperature or higher; the appearance of subsequent peaks then indicates distinct types of adsorption taking place on the same sites.

It is interesting to note the similarities in these TPD spectra and those obtained by Amenomiya and Pleizier (*35*) for hydrogen on a promoted iron catalyst. Their peaks identified as H(III) and H(IV) which appeared at approximately 373 and 473 K after adsorption at 873 K seem to be matched by those observed here at 393 and 453 K after adsorption at 775 K.

Badilla-Ohlbaum *et al.* (*25*) observed a maximum in the benzene hydrogenation rate over singly promoted iron catalyst at about 453 K and suggested that the H(IV) of Amenomiya and Pleizier (*35*) might be the hydrogen species involved in the surface reaction. It seems similarly significant in this work that both a TPD peak and the rate maximum were observed at 453 K.

Further work on the TPD spectra is in progress.

ACKNOWLEDGMENTS

Financial support from the National Research Council of Canada is gratefully acknowledged.

REFERENCES

1. Candy, J. P.,and Fouilloux, P., *J. Catal.* **38,** 110 (1975).
2. Evzerikhin, R. I., and Lyubarskii, G. D., *Kinet. Katal.* **7,** 934 (1966).
3. Germain, J. E., Maurel, R., Bourgeois, Y., and Sinn, R., *J. Chem. Phys.* **60,** 1219 (1963).
4. Herbo, C., *Bull. Soc. Chim. Belg.* **50,** 257 (1941).
5. Jiracek, F., Pacek, H., and Horak, J., *Collect. Czech. Chem. Commun.* **33,** 3211 (1968).
6. Kehoe, K. P. G., and Butt, J. B., *J. Appl. Chem. Biotechnol.* **22,** 23 (1972).
7. Motard, R. L., Burke, R. F., Canjar, L. N., and Beckman, R. B., *J. Appl. Chem. (London)* **7,** 1 (1957).
8. Snagovskii, Yu.S., Lyvbarskii, G. D., and Ostrovskii, G. M., *Kinet. Katal.* **7,** 232 (1966).
9. van Meerten, R. Z. C., and Coenen, J. W. E., *J. Catal.* **37,** 37 (1975).
10. Thomas, C. L., "Catalytic Processes and Proven Catalysts." Academic Press, New York, 1970.
11. Hartog, F., Tebben, J. H., and Zwietering, P., *Actes Congr. Int. Catal. 2nd 1960* **1,** 1229 (1961).
12. Nicolai, J., Martin, R., and Jungers, J. C., *Bull. Soc. Chim. Belg.* **57,** 555 (1948).
13. Roethe, K. P., Roethe, A., Rosahl, B., and Gelbin, D., *Chem. Ing. Tech.* **42,** 805 (1970).
14. Aben, P. C., Platteeuw, J. C., and Stouthamer, B., *Proc. Int. Congr. Catal. (Moscow) 1968,* p. 543 (pap. 31).
15. Coenen, J. W. E., van Meerten, R. Z. C., and Rijnten, H. T., *Proc. Int. Congr. Catal. 5 (Palm Beach, Fl) 1972* **1,** 671 (1973).
16. Dixon, G. M., and Singh, K., *Trans. Faraday Soc.* **65,** 1128 (1969).
17. Lyubarskii, G. D., *Actes Congr. Int. Catal. 1960* **1,** 1242 (1961).
18. Zlotina, N. E., and Kiperman, S. L., *Kinet. Katal.* **8,** 337, 1129 (1967).
19. Bond, G. C., "Catalysis by Metals." Academic Press, New York, 1962.
20. Herbo, C., and Hauchard, V., *Bull. Soc. Chim. Belg.* **52,** 35 (1943).
21. Herbo, C., *J. Chim. Phys.* **47,** 454 (1950).
22. Herbo, C., and Hauchard, V., *Bull. Soc. Chim. Belg.* **55,** 177 (1946).
23. Polanyi, M., and Greenhalgh, R. K., *Trans. Faraday Soc.* **35,** 520 (1939).
24. Madden, W. F., and Kemball, C., *J. Chem. Soc.* **54,** 302 (1961).
25. Badilla-Ohlbaum, R., Neuberg, H. J., Graydon, W. F., and Phillips, M. J., *J. Catal.* **47,** 273 (1977).
26. Kubicka, H., *J. Catal.* **12,** 223 (1968).
27. Nagata, S., Gasimoto, K., Tanama, I., Nisida, Kh., and Ivane, S., *Kagaku Kogaku* **27,** 558 (1963).
28. Canjar, L. N., and Manning, F. S., *J. Appl. Chem.* **12,** 73 (1962).
29. van Meerten, R. Z. C., and Coenen, J. W. E., *J. Catal.* **46,** 13 (1977).
30. Yates, D. J. C., Taylor, W. F., and Sinfelt, J. H., *J. Am. Chem. Soc.* **86,** 2996 (1964).
31. Beveridge, G. S. G., and Schechter, R. S., "Optimization Theory and Practice," pp. 396–406. McGraw-Hill, New York, 1970.
32. Rosenbrock. H. H., *Computer J.* **3,** 175–184 (1960).
33. Barbenics, L., and Tetenyi, P., *J. Catal.* **17,** 35 (1970).

34. Basset, J. M., Dalmai-Imelik, G., Primet, M., and Mutin, R., *J. Catal.* **37**, 22 (1975).

35. Amenomiya, Y., and Pleizier, G., *J. Catal.* **28**, 442 (1973).

36. Cvetanovic, R. J., and Amenomiya, Y., *in* "Advances in Catalysis" (D. D. Eley, H. Pines, and P. B. Weisz, Eds.), Vol. 17, p. 103. Academic Press, New York, 1967.